Reviewer #1:

Comments and Suggestions for Authors:

This manuscript reports lidar observations of an event with CBL as deep as over 5 km at the southern edge of the Taklimakan Desert. ERA5 reanalysis data was used to analyze the responsible mechanisms, as complemented by a conceptual diagram. The presented case is interesting and fits the scope of 'Measurement report' in ACP. I believe this work may be published upon addressing the issues given below.

Thanks a lot for your recognition of this work and for your carefully review. The manuscript has been greatly improved with your comments.

1. More discussions on the status of research on CBL should be given. Since this work aims to report an extreme CBL case, it is of necessity to give some background information on this point. For example, why the deep CBL is important? What are the known mechanisms contributing to deep CBL? Which knowledge gap that this study aims to address?

Some recent works have reported such deep CBL cases over this region. To what extent this work advances our understanding on the formation mechanism of deep CBL? This point will stand upon well addressing recent progresses regarding this topic.

Response: Thank you for pointing out these problems in the manuscript. We have added relevant background information to this manuscript.

Firstly, we have summarized the importance of studying deep CBL in the existing references, highlighting the necessity of conducting local studies on deep CBL. For example, "These studies also revealed that the deep CBL exerts an influence on the local pollutant transmission and diffusion, cloud formation processes, strong convective weather, rainfall, drought and so on", "However, the MinFeng station, which is located on the northern slope of the Tibet Plateau (TP) and has severe wind-sand activities (Yang et al., 2016; Xiao et al., 2008), was established in 2018 (Yang et al., 2020). On the one hand, there is a lack of sufficient study results of deep CBL, and the particularity of geographical locations (TD, slope terrain, Kunlun Mountains, TP) further complicates the formation mechanism of deep CBL. On the other hand, the deep CBL plays an important role in the regional circulation and weather, its study not only helps to reveal the mechanism of local dust emission and transport (Jia et al., 2015; Meng et al., 2019), but also promotes the understanding of the land-atmosphere interaction between the TD and the TP".

Secondly, we have introduced the existing mechanism of forming deep CBL in the Taklimakan Desert. For example, "in the hinterland of the TD, the intense surface heating is not the primary reason for the formation of deep CBL, whereas the presence of weak temperature inversion and near-neutral residual layer (RL) above the CBL are crucial (Zhang et al., 2022; Xu et al., 2018); The low-level jet (LLJ) can trigger significant air accumulation and dynamic convergence in the lower-level atmosphere, while the deep CBL is usually accompanied by the LLJ on the following night (Wang et al., 2019); The deep CBL enables the formation of clouds in the late afternoon, the formation of clouds will not only lead to a significant cooling of surface, but also make the momentum in the upper part of the boundary layer to transport downward and cause dust emissions (Zhang et al., 2024)".

Finally, in the conclusion part of the manuscript, we have summarized the key differences between the deep CBL formation mechanism presented in this study and those found in previous research. Previous studies have primarily concentrated on individual aspects, such as thermal or dynamic processes, to explain the formation of deep CBL. The formation of deep CBL in this

manuscript is a comprehensive effect of multiple factors under complex terrain (Taklimakan Desert, Tibet Plateau, slope terrain, Kunlun Mountains), including downhill airflow, low-level jet, inversion layer, the sensible heat driven air-pump from the Tibet Plateau, furnace effect, the atmospheric superadiabatic expansion process, cloud, and so on.

Change: P2L13-15. "These studies also revealed that the deep CBL exerts an influence on the local pollutant transmission and diffusion, cloud formation processes, strong convective weather, rainfall, drought and so on".

P2L16-30. "For example, in the hinterland of the TD, the intense surface heating is not the primary reason for the formation of deep CBL, whereas the presence of weak temperature inversion and near-neutral residual layer (RL) above the CBL are crucial (Zhang et al., 2022; Xu et al., 2018); The low-level jet (LLJ) can trigger significant air accumulation and dynamic convergence in the lower-level atmosphere, while the deep CBL is usually accompanied by the LLJ on the following night (Wang et al., 2019); The deep CBL enables the formation of clouds in the late afternoon, the formation of clouds will not only lead to a significant cooling of surface, but also make the momentum in the upper part of the boundary layer to transport downward and cause dust emissions (Zhang et al., 2024). Due to the fact that the TaZhong station is located in the center of the TD, and is equipped with the most comprehensive observation equipment, most studies of deep CBL are concentrated here. However, the MinFeng station, which is located on the northern slope of the Tibet Plateau (TP) and has severe wind-sand activities (Yang et al., 2016; Xiao et al., 2008), was established in 2018 (Yang et al., 2020). On the one hand, there is a lack of sufficient study results of deep CBL, and the particularity of geographical locations (TD, slope terrain, Kunlun Mountains, TP) further complicates the formation mechanism of deep CBL. On the other hand, the deep CBL plays an important role in the regional circulation and weather, its study not only helps to reveal the mechanism of local dust emission and transport (Jia et al., 2015; Meng et al., 2019), but also promotes the understanding of the land-atmosphere interaction between the TD and the TP".

P14L14-18. "The results indicate that the formation of this deep convective boundary layer stems from the combined effects of multiple factors under complex terrain, including the Taklimakan Desert, slope terrain, the Kunlun Mountains, and the Tibet Plateau. The primary factor is the low-level jet and inversion layer, which provide sufficient momentum, energy, and material prerequisites for the development of the atmospheric boundary layer. Furthermore, the thermal effect facilitates the formation of the deep convective boundary layer".

2. It is expected that the readers can reproduce your results after reading the Methods section, while the processing of lidar data is not adequately illustrated here.

Response: Thank you for your suggestion. We have introduced the data processing method of CDWL in the Appendix B of the manuscript, and the calculation of TKEDR is described in detail.

Change: P4L20-P5L9. "Based on this, the TKEDR threshold method can effectively estimate the BLH (Wang et al., 2021; Banakh et al., 2021).

The calculation formula of TKEDR is as follows (Banakh and Smalikho, 2018):

$$TKEDR = \left[\frac{\overline{D}_L(\varphi_l)-\overline{D}_L(\varphi_1)}{A(l\Delta y_k)-A(\Delta y_k)}\right]^{\frac{3}{2}} \quad (1)$$

where $\overline{D}_L(\varphi_l)$ is azimuth structure function, L is the serial number for the laser beam's line of sight. $\varphi_l = l\Delta\theta$, $\Delta\theta$ is the azimuth angle resolution, and l=1,2,3…. The $A(l\Delta y_k)$ is calculated theoretically for the Kolmogorov model of the two-dimensional turbulence spectrum (Banakh et al., 2017), Δy_k is the

transverse dimension of the probed volume, and k is the range gate number, k=1,2,3…. The error analysis for calculating TKEDR and BLH was conducted by Viktor A. Banakh (Banakh et al., 2017; Banakh et al., 2021).

In this experiment, the value of l is set to 2, and the threshold of TKEDR is set to 10^{-4} m^2 s^{-3}. When the location is at the height of H_n=ΔR*N (N is the index number of bins, and ΔR is radial spatial resolution), if all TKEDR values within the range [ΔR*(N+1), ΔR*(N+5)] are less than the threshold, then H_n is used as the BLH".

P18L6-P19L1. "The CNR is obtained by the ratio of the signal area to the noise area of the power spectrum (Fujii and Fukuchi, 2005):

$$CNR = A_s/A_n \quad \text{(B1)}$$

where A_s is the signal area of the power spectrum, A_n is the noise area of the power spectrum.

The line of sight velocity (V_{los}) of CDWL is given by the following formula:

$$V_{los} = \lambda f_i/2 \quad \text{(B2)}$$

where λ is the central wavelength of the emitted laser, f_i is the Doppler frequency shift for aerosols.

The wind vector in the atmosphere can be expressed by $\vec{V}$:

$$\vec{V} = (u, v, w) \quad \text{(B3)}$$

u, v, w represent the north-south velocity, east-west velocity, and vertical velocity, respectively.

When using Velocity Azimuth Display (VAD) scanning mode, the direction vector $\vec{S}$ can be expressed as:

$$\vec{S} = (cos\theta cos\varphi, sin\theta cos\varphi, sin\varphi) \quad \text{(B4)}$$

Where θ is the azimuth angle of the laser beam, and φ is the elevation of the laser beam.

From formula B2, B3, and B4, it can be concluded that (Browning and Wexler, 1968):

$$V_{los} = \vec{V} \cdot \vec{S}_m \quad \text{(B5)}$$

From formula B5, u, v, w can be calculated. The horizontal wind direction is calculated as follows:

$$WD = arctan\,(u, v) \quad \text{(B6)}".$$

3. The impact of clouds is not well discussed. The presence of clouds may partially block the solar radiation to surface. The observed clouds seem to be rather thin in Figure 3, and the vertical air motions of clouds are similar to the dust layer below. The discussion around P7L11 is rather vague.

Response: Thank you for pointing out the shortcomings in the manuscript, we have made a lot of improvements to the manuscript. Firstly, in Figure 3(c), the height of the cloud base has been marked with a purple dotted line based on the HWCT (Haar wavelet covariance transform) method. Secondly, in Appendix A3, the cloud coverage of the Taklimakan Desert was drawn using the Fengyun-4A meteorological satellite. Finally, we discussed the impact of clouds from four aspects in the manuscript.

The first is the distribution of clouds. For example, "Before 18:00 LT, the study site was covered by scattered clouds, and after 18:00 LT, the cloud completely covered the study site".

The second is the radiative cooling effect of clouds. For example, "The presence of clouds can greatly weaken the solar radiation reaching the surface, causing the surface temperature to decrease rapidly (Fig. 3a)", "When the cloud completely covered the study site, the surface radiation further cooled the near-surface air, greatly weakening the atmospheric turbulence intensity and significantly reducing the CBL height before sunset, and the ground-air temperature difference changed to -0.6 °C at 22:00 LT".

Then the cloud caused the change of atmospheric turbulence intensity. For example, "and gradually weakening the turbulence intensity of the atmosphere (Fig. 3c)", "At 17:00 LT~20:00 LT, the

atmospheric turbulence remained active during the initial stages of cloud formation".

Finally, the formation of upper-level cold front was promoted. For example, "the cold clouds moved towards the warm air mass over the desert, promoting the formation of an upper-level cold front and causing strong convective motion in the lower atmosphere (Fig. 3d), and the height of deep CBL reached its peak at 18:00 LT (Fig. 3c)".

In the aspects of the vertical movement of clouds and dust. On the one hand, due to the attenuation of the lidar signal by the cloud layer, most of the detected clouds are near the cloud base. On the other hand, during the early stages of cloud formation, the movement of cold clouds towards the warm air over the desert triggers intense convective motion in the lower atmosphere, resulting in similar vertical movements between the clouds and dust particles. However, after 20:00 LT, the vertical motion of the upper layer, which is higher than 5 km, is significantly greater than that of the lower layer.

Change: P7L19-29. "the study site began to be covered by clouds (Fig. 3c, Fig. A3). Before 18:00 LT, the study site was covered by scattered clouds, and after 18:00 LT, the cloud completely covered the study site. The presence of clouds can greatly weaken the solar radiation reaching the surface, causing the surface temperature to decrease rapidly (Fig. 3a), and gradually weakening the turbulence intensity of the atmosphere (Fig. 3c). At 17:00 LT~20:00 LT, the atmospheric turbulence remained active during the initial stages of cloud formation. On the one hand, as the surface temperature was still much higher than the atmospheric temperature, and the heat preservation effect of dust on the atmosphere continued to provide energy for the upper atmosphere. On the other hand, the cold clouds moved towards the warm air mass over the desert, promoting the formation of an upper-level cold front and causing strong convective motion in the lower atmosphere (Fig. 3d), and the height of deep CBL reached its peak at 18:00 LT (Fig. 3c). When the cloud completely covered the study site, the surface radiation further cooled the near-surface air, greatly weakening the atmospheric turbulence intensity and significantly reducing the CBL height before sunset, and the ground-air temperature difference changed to -0.6 °C at 22:00 LT".

P7L34. "The cloud coverage over the Taklimakan Desert is shown in Fig. A3".

P8L4-5. "and the cloud base height is marked with a purple dotted line".

P14L5-10. "As shown in Fig. 7(m-o), the relative humidity sinks from top to bottom above 4 km, while over the study site it gradually increases. Fig. A4n, on the other hand, shows the rapid drop in temperature over the desert caused by the invasion of cold air. The cold air invaded the TD and intersected with the warm air over the desert to form an upper-level cold front, and the cold air sank to force the desert basin to produce a strong convective motion (Fig. 7d, Fig. 7e, also analyzed in Sect. 3). At about 18:00 LT, with the participation of the upper-level cold front, the height of deep CBL reached its peak (Fig. 3c, Fig. 6(28), Fig. 7s)".

P16L9. "The cloud coverage over the Taklimakan Desert is shown in Fig. A3".

P17L5-6. "Figure A3. The cloud coverage over the Taklimakan Desert recorded by the Fengyun-4A Meteorological Satellite of China on 6 June, 2022 (UTC+8).".

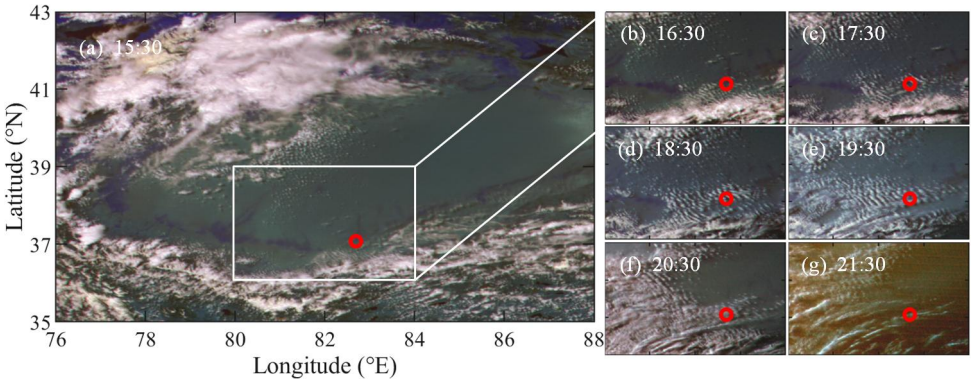

Figure A3. The cloud coverage over the Taklimakan Desert recorded by the Fengyun-4A Meteorological Satellite of China on 6 June, 2022 (UTC+8).

4. Causality issue. One of the major conclusions is that LLJ plays an important role in forming deep CBL. I do see that the study site was in the LLJ region, however, I did not find strong evidence showing how LLJ contributes to the formation of deep CBL in section 4.1. At the very least, one may be convinced if you show the well correlated time series of LLJ and BLH. Therefore, I suggest the authors to reorganize this section, and discuss this point more concisely and logically.

Response: Thanks for your kind reminder. We have added some descriptions of the role of LLJ in the development of deep CBL in section 4.1. For example, "In summary, the LLJ formed a water vapor convergence area in front of the study site and maintained the temperature within a relatively high range (16°C isotherm), which enhanced the potential instability (Fig. 4(g-i)), thereby strengthening the convective potential of the atmosphere and providing the necessary energy and water vapor conditions for the subsequent development of the boundary layer", "At the study site, the atmospheric temperature change caused by the LLJ promoted the formation of the IL, and the most obvious IL phenomenon was observed at 8:00 LT. The IL can weaken the convective motion of atmosphere, resulting in the boundary layer height near the study site being constrained within 0.25 km, thereby limiting the diffusion and mixing of dust pollutants, and serving as a source of dust material for further boundary layer development".

However, in section 3, the importance of LLJ to the formation of deep CBL has been fully demonstrated through lidar data. At the same time, the corresponding relationship between BLH and LLJ was also given in time series (Fig.3b and Fig.3c). Therefore, in Section 4.1, the causes and development of the LLJ in this area were mainly discussed, and the correctness of the CDWL observation was also confirmed. In addition, it is worth noting that the spatial resolution of ERA5 is 0.25°×0.25°, and the temporal resolution is 1 hour, which makes it difficult to study the spatiotemporal behavior of the CBL of this day at the study site.

Change: P9L10. "As seen in the wind vector subgraphs".

P9L10-11. "thus confirming the validity of observing LLJ using CDWL".

P10L8-11. "In summary, the LLJ formed a water vapor convergence area in front of the study site and maintained the temperature within a relatively high range (16°C isotherm), which enhanced the potential instability (Fig. 4(g-i)), thereby strengthening the convective potential of the atmosphere and providing the necessary energy and water vapor conditions for the subsequent development of the boundary layer".

P11L9-13. "At the study site, the atmospheric temperature change caused by the LLJ promoted the

formation of the IL, and the most obvious IL phenomenon was observed at 8:00 LT. The IL can weaken the convective motion of atmosphere, resulting in the boundary layer height near the study site being constrained within 0.25 km, thereby limiting the diffusion and mixing of dust pollutants, and serving as a source of dust material for further boundary layer development".

5. From Fig.8b, it seems that the cold front is tangentially related to the deep CBL. Looking back to the discussion at P13L23, I am not sure how the processes could be interpretated from the figure given.

Response: Thank you for your question, we further revised the manuscript. We have added Fig. A4 in Appendix A to show the temperature variations at different heights. Firstly, from Fig. A4n, it can be found that the cold air moving with the cloud greatly cooled the upper part of the study site. Secondly, in Fig. 7(m-o), the relative humidity sinks from top to bottom above 4 km. Thirdly, in Fig. 3d, Fig.7d, and Fig.7e, the cold air mass actively moves towards the warm air mass over the desert, thus forcing the desert basin to produce a strong convective motion. Finally, with the participation of the upper-level cold front, the height of the boundary layer reached its peak at approximately 18:00 LT.

Change: P7L25-27. "On the other hand, the cold clouds moved towards the warm air mass over the desert, promoting the formation of an upper-level cold front and causing strong convective motion in the lower atmosphere (Fig. 3d), and the height of deep CBL reached its peak at 18:00 LT (Fig. 3c)."

P7L34. "The cloud coverage over the Taklimakan Desert is shown in Fig. A3".

P14L5-10. "As shown in Fig. 7(m-o), the relative humidity sinks from top to bottom above 4 km, while over the study site it gradually increases. Fig. A4n, on the other hand, shows the rapid drop in temperature over the desert caused by the invasion of cold air. The cold air invaded the TD and intersected with the warm air over the desert to form an upper-level cold front, and the cold air sank to force the desert basin to produce a strong convective motion (Fig. 7d, Fig. 7e, also analyzed in Sect. 3). At about 18:00 LT, with the participation of the upper-level cold front, the height of deep CBL reached its peak (Fig. 3c, Fig. 6(28), Fig. 7s).".

P16L9-10. "Fig. A4 shows temperature variations at different altitudes over the Taklimakan Desert".

P18L2-4. "Figure A4. Temperature variations over the Taklimakan Desert during the period from 12:00 LT to 18:00 LT (UTC+8), observed at different atmospheric pressures or heights. The height represents the height from the ground at the study site. The purple circle represents the study site.".

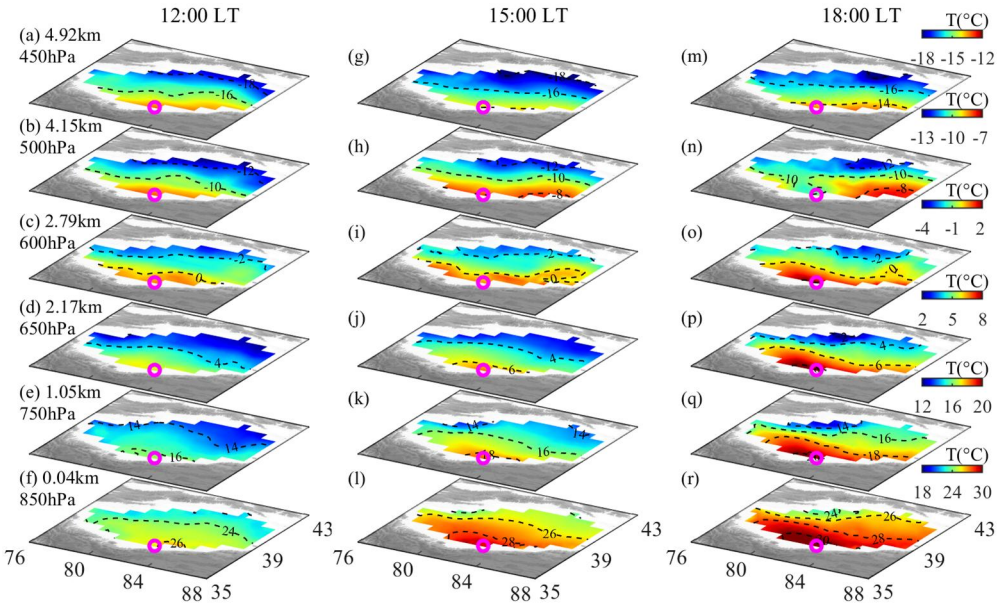

Figure A4. Temperature variations over the Taklimakan Desert during the period from 12:00 LT to 18:00 LT (UTC+8), observed at different atmospheric pressures or heights. The height represents the height from the ground at the study site. The purple circle represents the study site.

6. ACP usually has very good production team, but I would suggest to find a native speaker to improve the language issues. Some awkward expressions may be revised.

Response: Thank you for your kind reminder, we have carefully revised the English language. All changes made in the revised manuscript are marked in blue.

Change: P1L17-18. "During the stage of LLJ prior to the formation of the deep CBL, the LLJ had made sufficient preparations for the development of the deep CBL in terms of momentum, energy, and material".

P1L20. "temperature inversion layer".

P1L22. "During the stage of thermal effects, During the stage of thermal effects, the sensible heat driven air-pump from the Tibet Plateau".

P3L1. "In the detection of the BLH".

P3L2-6. "These characteristics of CDWL enable it to obtain the air flow conditions of the atmosphere from the calculated wind field information, monitor the change of the BLH in real time and more accurately, and help to understand the diffusion and retention of dust pollutants. Overall, the CDWL can be used for long-term continuous and stable detection in desert areas, and it is one of the effective ways to estimate the BLH in the desert".

…